

Review

Research status and prospect of alloying properties of Al-Zn-Mg-Cu series aluminum alloy

Jue Wang and Faguo Li *

School of Materials Science and Engineering, Xiangtan University, Xiangtan 411105, China;
wj200204032022@163.com (J.W.)

* Correspondence author: lifaguo@xtu.edu.cn (F.L.)

Abstract: Al-Zn-Mg-Cu alloy has high specific strength, good corrosion resistance, fracture toughness and fatigue resistance. It is one of the most important structural materials in the fields of aviation, aerospace, weapons, transportation and so on, which plays a huge role in the field of aerospace. In order to optimize the strength, toughness and corrosion properties of Al-Zn-Mg-Cu alloy, alloying has always been the focus of research on Al-Zn-Mg-Cu alloy. The effects of main alloying elements, trace alloying elements and rare earth elements on the microstructure and properties of Al-Zn-Mg-Cu aluminum alloy were briefly introduced in the paper, and the future research directions were prospected.

Keywords: Al-Zn-Mg-Cu alloying; main alloy elements; Microalloy elements; rare earth element; performance optimization

1. Introduction

The main elements of Al-Zn-Mg-Cu alloy include Al, Zn, Mg and Cu, which contain trace amounts of Si and Fe (usually present as impurity elements). The types and contents of trace elements are different among different brands, which leads to the different mechanical properties of the alloy. Therefore, the mechanical properties of the alloy could be improved by adjusting the composition of Al-Zn-Mg-Cu alloy, selectively introducing trace alloying elements, reducing the impurity content and realizing the reasonable distribution of precipitated phase. Rare earth elements played a more significant role in this process due to their special electronic structure and chemical properties. Therefore, it is of great significance for further strengthening and toughening Al-Zn-Mg-Cu alloy to explore the influence mechanism of different elements on the properties of the alloy, seek the action range and the optimum content of elements.

Main alloy elements

The main alloying elements in Al-Zn-Mg-Cu alloy are Zn, Mg and Cu. MgZn₂ phase is the main strengthening phase in aluminum alloy, and the increase of Zn and Mg elements could improve the yield strength of the alloy. Cu had a certain contribution to the strength of the alloy that improved the corrosion resistance. But there was a threshold for each element, for which the difference is obvious for different components of alloys.

1.1. Cu

Cu had a certain strengthening effect in Al-Zn-Mg-Cu alloys that had a prominent effect on the corrosion resistance of the alloys. The addition of Cu could improve the aging hardening potential of the alloy and increase the density of the precipitated strengthened phase [1], but excessive Cu would reduce the solid solubility of Zn and Mg in the aluminum alloy, which resulted in a decrease in the volume fraction of MgZn₂ strengthened phase. Therefore, reducing the contents of Cu in a certain range was conducive to the diffusion of more Zn and Mg into the matrix, and increase the volume

fraction of strengthening phase $\text{Mg}(\text{Zn}, \text{Al}, \text{Cu})_2$, thus improving the Yield strength (YS) and hardness of the alloy.

The effect of Cu on the properties of Al-Zn-Mg-Cu alloy was related to the alloy composition. In low Zn/Mg ratio alloys (such as type 7050), the addition of Cu increased the amount of reinforced precipitated phase and improved the yield strength and corrosion resistance of the alloy. However, in Al-9.3Zn-2.4Mg-xCu-0.16Zr aluminum alloy with high Zn/Mg ratio, the mechanical properties of the alloy were improved with the decrease of Cu content (Figure 1a) when the Cu content decreases from 2.2% to 1.8% (mass fraction), and the resistance to spalling corrosion was also significantly improved. When the Cu content was reduced to 0.8% (mass fraction), the potential difference between the grain boundary and Al matrix became larger, which resulted in corrosion of the precipitated phase and deteriorated the corrosion performance significantly (Figure 1b) [2].

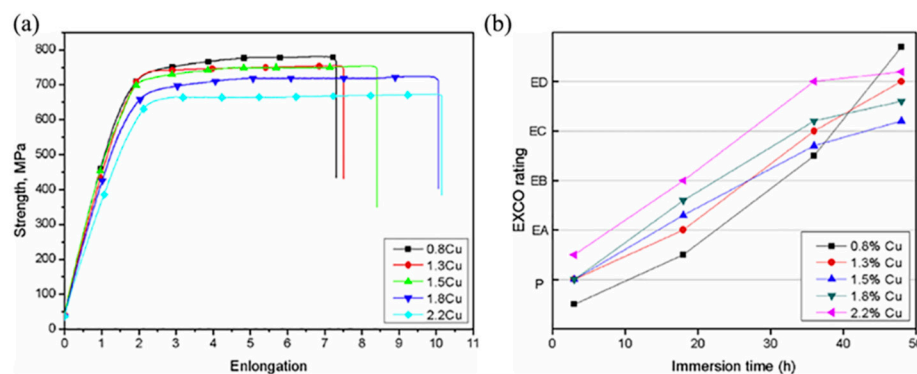


Figure 1. Stress-strain curves (a) of Al-9.3Zn-2.4 Mg-xCu-Zr alloy and evolution of the EXCO rating as a function of immersion time for the alloys in the T6 heat treatment (b) [2].

In highly alloyed Al-Zn-Mg-Cu alloy, the influence of Cu element on the comprehensive properties included grain refinement and coupling effect of residual eutectic phase. In Al-10.0Zn-2.6Mg-xCu-0.15Zr alloys, on the one hand, the volume fraction of the second phase increased significantly with the increase of Cu content. On the other hand, the low diffusion coefficient of Cu inhibited the dissolution of the second phase, which made the volume fraction of the residual eutectic phase gradually increase after solid solution. The hard and brittle residual eutectic phase was easy to cause stress concentration and became a crack source, which seriously damaged the plasticity of the alloy. For Al-10.0Zn-2.6Mg-1.0Cu alloy with $x=1.0$, the precipitated phase was small and the volume fraction was large, which had the best mechanical properties [3].

1.2. Mg

Mg was the main strengthening element of Al-Zn-Mg-Cu alloy. $\text{H} (\text{MgZn}_2)$ phase formed by Mg and Zn had a large solid solubility in the matrix and decreased significantly with the decrease of temperature, which had a strong aging hardening ability and was the main strengthening phase of Al-Zn-Mg-Cu alloy. With the increase of Mg content, $\alpha(\text{Al})$ grains were refined and tertiary dendrites and $\text{T}(\text{AlCuMgZn})$ phases increased [4]. In addition, the increase of Mg content could improve the volume fraction of precipitated phase during aging treatment, thus improving the yield strength [5]. However, high yield stress could also lead to lower deformation resistance at grain boundaries, thus promoting intergranular fracture and reducing plasticity [6].

1.3. Zn

In Al-Zn-Mg-Cu alloy, increasing Zn content in the alloy could promote the nucleation, growth and phase precipitation transformation of the alloy. Al-Zn-Mg-Cu alloy with high Zn content had high precipitation density and fast precipitation rate, which had the advantages of improving the alloy strength and shortening the peak aging time [7]. When the Zn content increased from 4.4%

(mass fraction) to 7.2% (mass fraction), the Ultimate tensile strength (UTS) of Al-xZn-2.3Mg-1.7Cu alloy increased from 212.15MPa to 248.05MPa, which increased by 16.92%; The Elongation (Elongation, EL) increased first and then decreased with the increase of Zn content. And the maximum elongation was 8.78% when $x=5.8$ [8]. The increase in the number of MgZn₂ strengthened phases and the change in the shape, number and size of intercrystalline eutectic phases improved the tensile strength. And the change in elongation was mainly due to the refinement of grain size and the transformation of dendrite morphology from columnar dendrite to cellular dendrite [9].

Zn had an important effect on the softening behavior of Al-Zn-Mg-Cu alloys. At 300 °C, there was a plateau in the static softening curve of the alloy. The increase of Zn content promoted the formation and coarsening of η phases, which also promoted the duration and softening fraction of the plateau decrease (Figure 2a,b). When the deformation temperature increased to 400 °C, the static softening curve was less affected by Zn content (Figure 2c,d) [10]. The effect of Zn content on dynamic softening behavior was shown in Figure 3. The increase of Zn led to the acceleration of work hardening at the initial deformation stage at 300 °C, and the dynamic softening process was enhanced with the increase of Zn content. However, at 400 °C, the high supersaturation solid solubility caused by the addition of Zn inhibited the dynamic recovery and recrystallization process, which resulted in a slow down of dynamic softening behavior (Figure 3c,d) [11].

The hot-cracking sensitivity of Al-Zn-Mg-Cu alloy increased first and then decreased with the increase of Zn content. When the Zn content was 5% (mass fraction) and 11% (mass fraction), the hot-cracking sensitivity was low. And when the Zn content is 9% (mass fraction), the hot-cracking sensitivity was the highest [12]. The thermal cracking sensitivity of the alloy was determined by grain morphology, grain size, thermal shrinkage behavior of the solidification interval and non-equilibrium eutectic content. The increase of Zn content increased the thermal shrinkage of the alloy, which resulted in a larger thermal strain during the solidification process. Although the decrease of grain size helped to reduce the thermal cracking sensitivity of the alloy, the transition from equiaxed spherules to irregular grains reduced the fluidity of the alloy. So the hot cracking sensitivity of the alloy with 9% Zn content (mass fraction) was the highest. When the content of Zn was further increased to 11% (mass fraction), the grain was refined and transformed from equiaxed crystal to fine dendrite and the thermal shrinkage rate increased. But the significant increase of the non-equilibrium eutectic content enabled the alloy to have a better ability to heal the cracks and begin to decrease the thermal crack sensitivity.

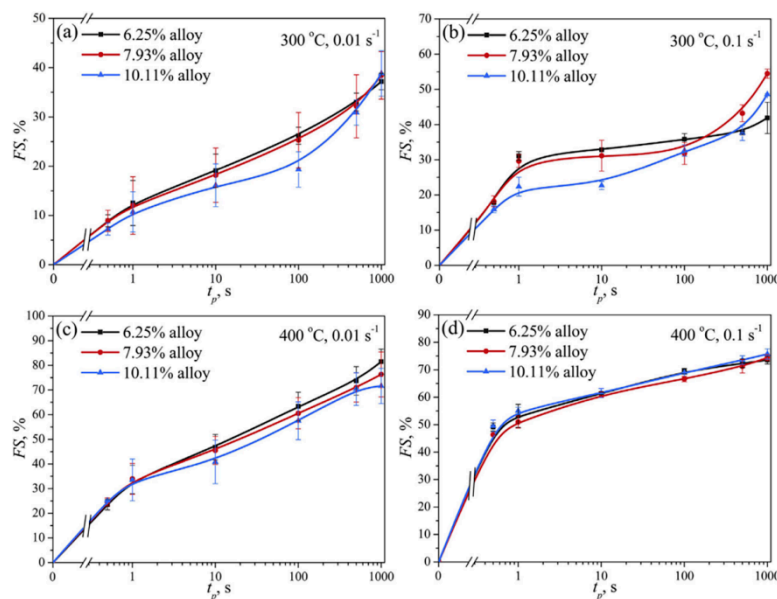


Figure 2. Static softening curves of Al-Zn-Mg-Cu alloy with different Zn contents under two-stage hot compression (a) 300 °C, 0.01 s⁻¹; (b) 300 °C, 0.1 s⁻¹; (c) 400 °C, 0.01 s⁻¹ and (d) 400 °C, 0.1 s⁻¹ [10].

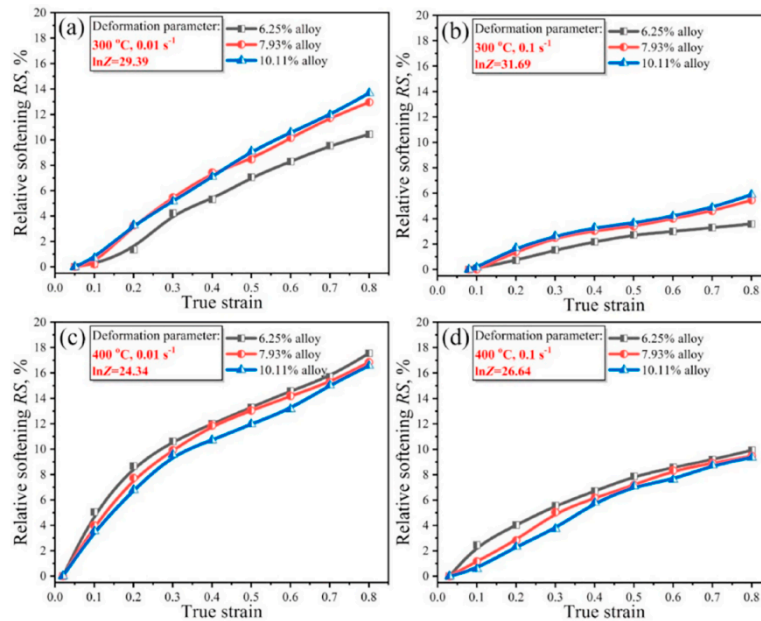


Figure 3. Relative dynamic softening behavior of Al-Zn-Mg-Cu alloys with different Zn contents during continuous compression (a) 300 °C, 0.01s⁻¹; (b) 300 °C, 0.1 s⁻¹; (c) 400 °C, 0.01 s⁻¹; (d) 400 °C, 0.1 s⁻¹ [11].

1.4. Cu/Mg ratio

Mg content was the main factor affecting the strength of over-aged Al-Zn-Mg-Cu alloy. The increase of Cu content could also enhance the strength, but to a lesser extent. In contrast, for spray formed aluminum alloy, the volume fraction of the secondary phase inside the grain was mainly determined by the Mg content, and the volume fraction of the secondary phase at the grain boundary was mainly controlled by the Mg+Cu content. After solid solution treatment, coarse grain boundary phase with high Mg content was difficult to enter the single-phase Al region, so the formation of refractory phase in Mg rich (2.65%, mass fraction) aluminum alloy could be promoted by adding Cu element, which was conducive to maintaining the peak strength of the alloy in the over-aging state [5]. In addition, it had been found that compared with non-Cu alloys, the yield strength of Al-4.0Mg-3.0Zn-1.5Cu aluminum alloys with high Cu increased by 80.5%, while the ductility does not decreased [13]. Therefore, a balance between ductility and strength was expected to be achieved by appropriate adjustment of Cu/Mg ratio.

The influence of Cu/Mg ratio on Al-Zn-Mg-Cu alloy was mainly reflected in two aspects: one was to affect the coarsening rate in the aging process; the other was to change the size and distribution of precipitated phase. Alloys with a low Cu/Mg ratio had a slow coarsening rate and a high tensile strength (Figure 4). Under T79 aging, Cu/Mg had the highest tensile strength than the lowest 2.5Mg1.5Cu alloy. The alloys with a higher Cu/Mg ratio had coarser Grain boundary precipitates, GBPs) and a wider Precipitate free zone (PFZ) could effectively delay the propagation of microcracks along grain boundaries [14]. With the increase of Cu/Mg ratio, the elongation of Al-Zn-Mg-Cu alloy increased significantly, and the fracture morphology changed from the typical brittle fracture to the intergranular mixed fracture or ductile fracture.

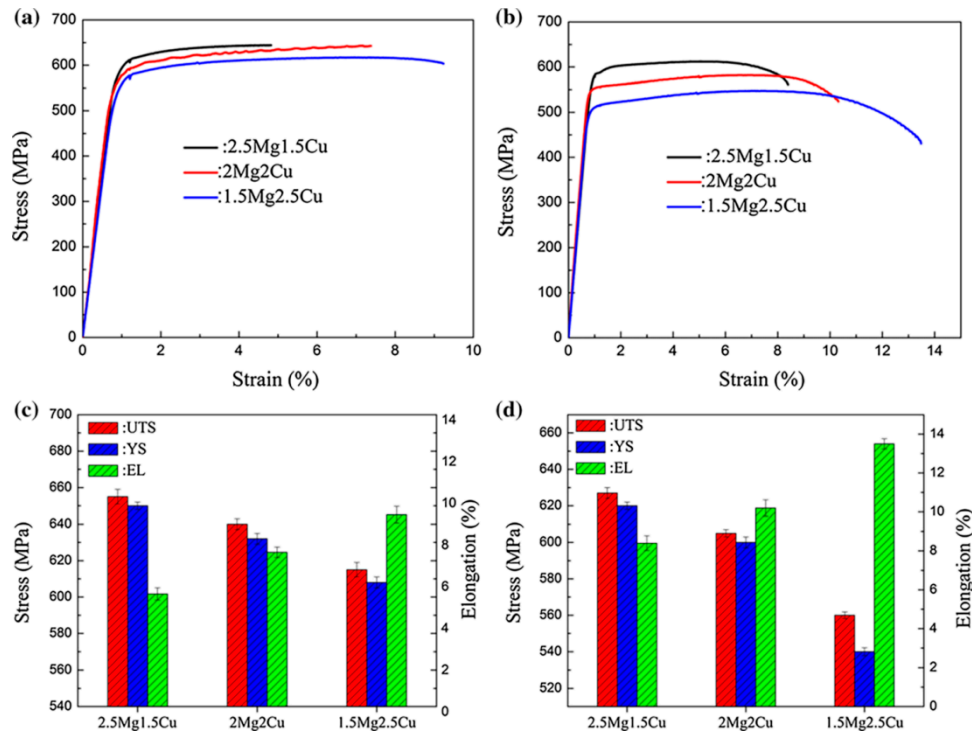


Figure 4. Mechanical properties for all alloys after T79 and T74 aging: (a, b) stress–strain curves after T79 and T74 aging, respectively, (c, d) UTS, YS and EL after T79 and T74 aging, respectively [14].

1.5. Zn/Mg ratio

The Zn/Mg ratio was closely related to the strength and stress corrosion resistance of Al-Zn-Mg-Cu alloy, and also affected the precipitation sequence and phase of the alloy. It was generally believed that the precipitation sequence of Al-Zn-Mg-Cu alloy was as follows: SSSS→GP region → η' phase → η' phase (MgZn_2) [15]. With the decrease of Zn/Mg ratio, T' phase replaces η' phase, and the precipitation sequence changed to SSSS→GPI region →GPII region → intermediate phase T'→ equilibrium phase T- $\text{Mg}_{32}(\text{Al,Zn})_{49}$ [16].

The influence of Zn/Mg ratio on mechanical properties of Al-Zn-Mg-Cu alloy was shown in Figure 5. As the Zn/Mg ratio increased from 1.50 to 2.86, the density and strength of precipitated phase in the alloy increased and more solute atoms precipitated at grain boundaries or within grains, which led to a decrease in PFZ width and elongation. When the Zn/Mg ratio further increased from 2.86 to 10.00, the changes in strength and elongation were opposite to those before [17]. In addition, the increase of Zn/Mg ratio could reduce the precipitation of equilibrium η phase during slow quenching, which resulted in the increase of enhanced precipitates after aging treatment, thus reducing the quenching sensitivity of the alloy [18]. For high Zn/Mg ratio alloys, the critical cooling rate without precipitation during the cooling process was about 100 K/s. While for low Zn/Mg ratio alloys, the critical cooling rate was about 1 K/s [19]. Therefore, Al-Zn-Mg-Cu alloys with high Zn/Mg ratio showed higher quenching sensitivity and were more prone to hot cracking.

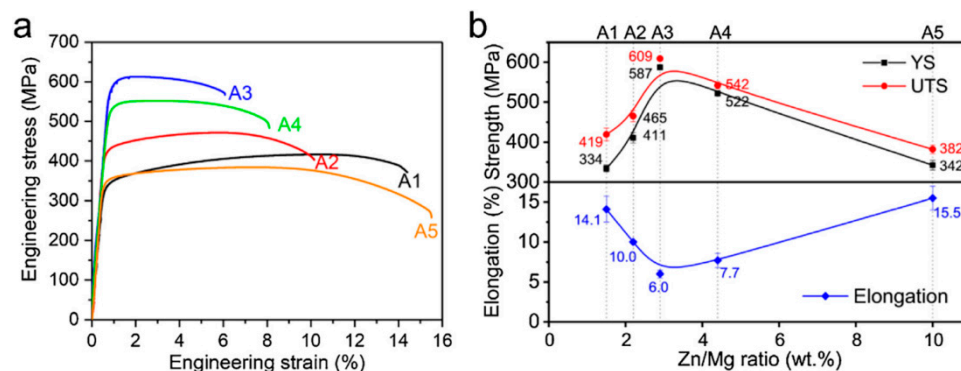


Figure 5. Mechanical properties of peak aged samples: (a) engineering stress–strain curves; (b) strength and elongation values as a function of Zn/Mg ratios [17].

The relationship between corrosion resistance of Al-Zn-Mg-Cu alloy and Zn/Mg ratio was shown in Figure 6. Electrochemical impedance spectroscopy (EIS) revealed the relationship between impedance size, phase Angle, and frequency. Electrochemical impedance spectroscopy (EIS) showed the relationship between electrochemical impedance, phase Angle, medium frequency range, and corrosion resistance of electrochemical impedance spectroscopy. With the increase of Zn/Mg ratio, the arc radius and phase Angle of Nyquist curve decreased, which indicated that the corrosion resistance of the alloy decreased [20]. And Al-Zn-Mg-Cu alloy with lower Zn/Mg ratio showed better surface protection and corrosion resistance [21].

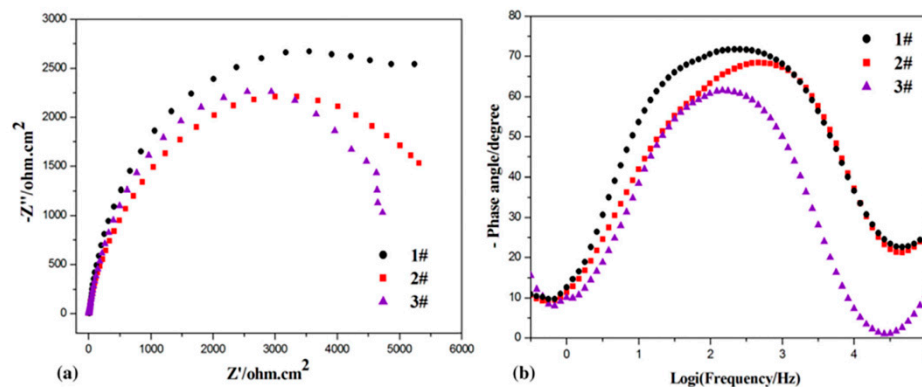


Figure 6. Electrochemical impedance spectroscopy response of the Al-Zn-Mg-Cu alloys with three different Zn/Mg ratios (in 3.5 wt.% NaCl solution): (a) Nyquist plot, (b) phase angle and frequency, (c) impedance and frequency (1#:3.46; 2#:3.84; 3#:4.04) [21].

2. Microalloy elements

Trace elements in Al-Zn-Mg-Cu alloys include two categories: first, they are impurity elements, mainly Fe and Si. A small amount of impurity elements inevitably existed in aluminum alloys and with the recycling of recycled aluminum, the content of Fe and Si in the alloys would further increase. The second is alloying elements including Ag, Ni, Ti, etc. Microalloying elements were mainly introduced to refine grain and improve alloy strength.

2.1. Fe, Si

Fe and Si were the most common impurity elements in Al-Zn-Mg-Cu alloys, and generally form coarse $\text{Al}_7\text{Cu}_2\text{Fe}$, Al_3Fe , $\alpha\text{-AlFeSi}$ and Mg_2Si phases in the alloys [22,23]. The brittle and hard $\text{Al}_7\text{Cu}_2\text{Fe}$ phase was not coherent with the $\alpha(\text{Al})$ matrix and was easy to crack or separate from the matrix to form voids. It grew up under the loading stress and eventually formed macroscopic cracks, which led to the fracture of the alloy [24].

When Fe content increased from 0.12% (mass fraction) to 0.26% (mass fraction), the tensile strength of the alloy changed little, where the elongation decreased seriously [25]. When Fe content increased from 0.0% (mass fraction) to 0.6% (mass fraction), the fracture toughness decreased from $40 \text{ MPa.m}^{1/2}$ to $30 \text{ MPa.m}^{1/2}$ [26]. However, the fatigue life of Al-Zn-Mg-Cu alloys could be improved by reasonable control of Fe content. When the strain amplitude was less than 0.5%, the fatigue life of Al-Zn-Mg-Cu alloy with 0.33% (mass fraction) Fe was obviously better than that with 0.01% (mass fraction) Fe [27]. The reason was that fine Fe-rich phase could change the crack propagation path under low strain amplitude and increased the crack propagation resistance, which greatly improved the fatigue life. However, when the volume fraction and size of the Fe-rich phase exceeded a certain critical value, the Fe-rich phase might still become a crack source, which would damage the fatigue property of the alloy.

The Al-4.5Zn-1.5Mg-1.0Cu-0.35Si alloy contained fine and dispersed plate-strip precipitates in the intragranular structure, which was called the GPB-II zone [28]. The GPB-II zone exhibited stronger stability than η' and T' phases under high temperature aging, which significantly improved the alloy strength [29]. After aging at 125°C, 175°C and 225°C, the microhardness and strength of Al-Zn-Mg-Cu alloys containing Si were significantly higher than those without Si.

Fe and Si could change the mechanical properties of Al-Zn-Mg-Cu alloy by influencing the recrystallization process. The change of grain boundary orientation distribution was closely related to recrystallization caused by Particle stimulated nucleation (PSN) of Al₇Cu₂Fe and Mg₂Si [30]. With the increase of Fe and Si content, the density of Al₇Cu₂Fe and Mg₂Si increased. It was easier to induce recrystallization and formed recrystallized grains whose orientation was much different from the texture direction of extruded fibers, which contributed to the formation of more high Angle grain boundaries. When the mass fraction of Fe and Si increased from 0.041% and 0.024% to 0.272% and 0.134%, respectively, Recrystallization resulted in a decrease in the texture of extruded fibers from 56.8% to 53.8% [31], which decreased slightly strength. High Angle grain boundaries hindered deformation more seriously and promote intergranular fracture more easily than low Angle grain boundaries. Therefore, with the increase of Fe and Si content, a large number of coarse Al₇Cu₂Fe and Mg₂Si phases and more high Angle grain boundaries would also reduce the elongation.

2.2. Ag

Ag could significantly improve the early aging response and the overall aging response of Al-Zn-Mg-Cu alloy [32], which increased the density of fine aggregates. The aggregate density of 7075 alloy after peak aging was $1.2 \times 10^{24} \text{ m}^{-3}$, which increased to $3.1 \times 10^{24} \text{ m}^{-3}$ after adding 0.3% Ag. The increase of fine T-phase and η phase density in Ag-containing alloys increased the hardness and yield strength by more than 10% [33].

The tensile strength of Al-4.5Zn-1.55Mg-0.12Cu alloy with 0.12% Ag added was 457.6 MPa in 3.5% NaCl solution, and it was 20.5 MPa higher than that without Ag added, which loss elongation little and showed better corrosion resistance to NaCl solution (Figure 7) [34]. On the one hand, Ag atoms were distributed around the grain boundary precipitated phase, which significantly reduced the potential difference between PFZ and GBPs, increased pitting potential, and reduced the sensitivity of the alloy to stress corrosion cracking. On the other hand, the addition of trace Ag could increase the size of precipitated phase and the distance between precipitated phases, which was conducive to the capture of hydrogen atoms in the grain boundary, so as to improve the stress corrosion resistance of the alloy.

When Ag was added to Al-Zn-Mg-Cu alloys containing Ge, a small amount of Ag could effectively capture vacancy and reduced vacancy loss near the grain boundary, which effectively reduced the width of PFZ. The joint addition of Ge and Ag made Mg₂Ge particles finer and more evenly distributed, which reduced the degree of stress concentration and further improved the plasticity of the alloy. After air cooling, the fracture changed from brittle intergranular fracture to ductile transgranular fracture (Figure 8) [35].

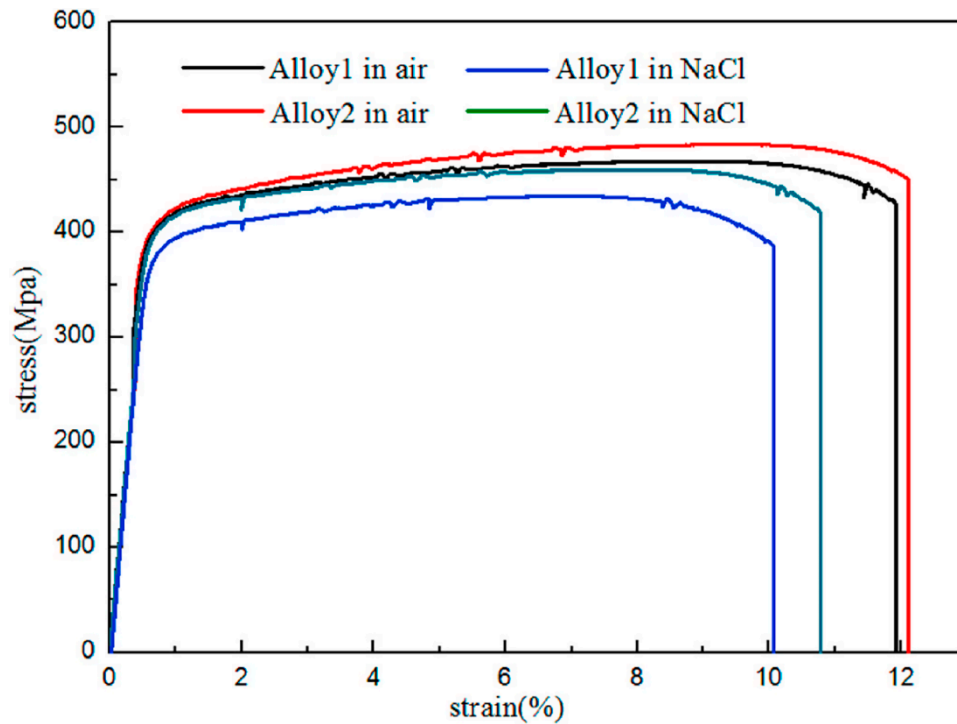


Figure 7. Stress-strain curves of the Al-4.5Zn-1.55Mg-0.12Cu alloys (Alloy 1: without Ag addition; Alloy 2: 0.12wt.% Ag) [34].

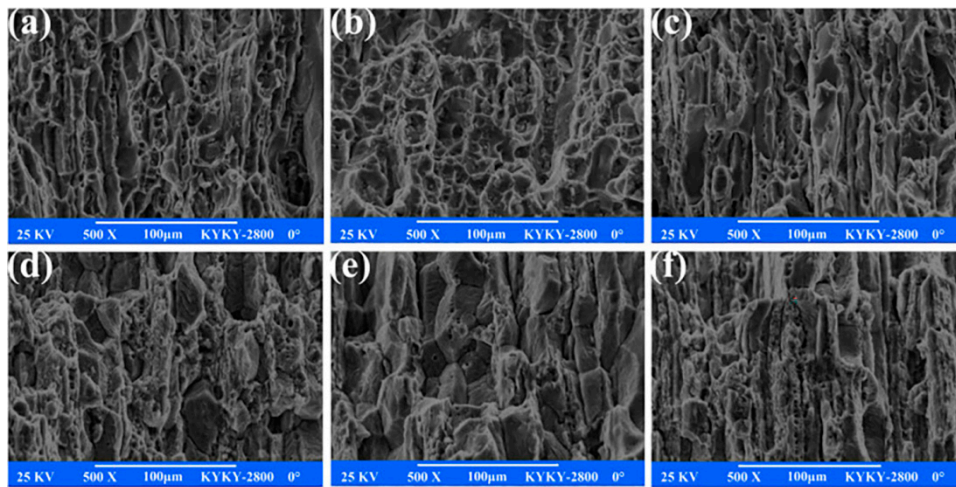


Figure 8. Scanning electron micrographs of fracture surfaces of tensile specimens of water quenching alloys (a-c) and air cooling alloys (d-f): (a, d) Base alloy; (b, e) Add Ge; (c, f) Add (Ge+Ag) [35].

2.3. Ni

It had been shown that adding Ni to Al alloy could improve the strength at room temperature or high temperature, which had been confirmed in Al-Zn-Mg-Cu alloy [36]. In the equilibrium phase diagram of Al-Zn-Mg-Cu-Ni alloy, Ni only existed in the form of (Al+Al₃Ni) eutectic [37]. Generally speaking, the increase of eutectic helped to inhibit the formation of hot cracking of casting alloy, which effectively reduced the hot cracking tendency of alloy.

In as-cast Al-Zn-Mg-Cu-Ni alloys, the amount of Al₃Ni phase increased with the increase of Ni content. The Al₃Ni phase was formed by $L \rightarrow (\alpha\text{-Al} + \text{Al}_3\text{Ni})$ eutectic reaction at the last stage of solidification. The increase of Al₃Ni phase on the fracture surface meant that there was more residual liquid between the primary $\alpha\text{-Al}$ dendrites. In this case, the initial fracture would be filled with residual eutectic liquid, which reduced the possibility of thermal cracking. When the amount of Ni was less than 0.6% (mass fraction), the improvement of grain size and shrinkage defect could improve

the tensile strength and elongation at the same time. However, when the Ni content was more than 0.6% (mass fraction), the increase of alloy strength led to the decrease of the elongation. When the Ni content was greater than 1.2% (mass fraction), the alloy had no hot cracking tendency [38]. Therefore, the strength and elongation of Al-Zn-Mg-Cu alloy could be increased by adding appropriate amount of Ni, and the thermal cracking sensitivity could be reduced, so as to improve the service performance of the material.

2.4. Ti

The effects of Ti on Hot tearing sensitivity (HTS) of Al-Zn-Mg-Cu alloys were related to the content of elements. Adding 0.06% (mass fraction) Ti could reduce the hot-cracking sensitivity factor of Al-6Zn-2Mg-2Cu-Ti alloy from 17 (0.00%Ti, mass fraction) to 7 (0.06%Ti, mass fraction). But with further increase of Ti content, the hot-cracking sensitivity factor increased from 7 (0.06%Ti, mass fraction) to 13 (0.24%Ti, mass fraction) [39], which reduced the pouring performance of the alloy.

In addition to affecting the hot-cracking sensitivity of the alloy, 0.1% (mass fraction) Ti could also reduce the grain size and the degree of phase agglomeration during the solidification of Al-Zn-Mg-Cu alloy, thus improving the strength and plasticity of the as-cast alloy. The addition of Ti changed the chemical composition of L₁₂ precipitated phase from (Al,Zn)₃Zr to (Al,Zn)₃(Zr,Ti), and the lattice constant decreased from 0.4111 nm to 0.4018 nm. Because the decrease of lattice constant resulted in the lattice mismatch between the precipitated phase and Al matrix, L₁₂ precipitated phase was refined from 18.7±0.4 nm to 14.2±0.4 nm [40]. In addition, the addition of Ti led to the formation of Al₁₈Mg₃Ti₂ metal compound phase during the solid solution process, which played an important role in the preferential nucleation of η-Mg(Zn,Cu,Al)₂ precipitates in slow-cooling alloys after solid solution treatment [41]. At the same time, the interface between Al₁₈Mg₃Ti₂ phase and Al matrix also provided non-uniform nucleation sites for L₁₂ precipitated phase and zinc-rich phase [42].

3. Rare earth element

The effects of rare earth elements on Al-Zn-Mg-Cu alloys were similar, which were mainly reflected in the following aspects: on the one hand, the solubility of rare earth elements in aluminum was small, and they could form Al₃RE phase with Al. In the solidification process, the Al₃RE phase served as the heterogeneous core of Al matrix, which significantly refined the grains. On the other hand, the dispersing Al₃RE phase was strongly pinned to the dislocation in the process of homogenization and solution aging, which effectively inhibited the recrystallization of the alloy and significantly increased the recrystallization temperature. In addition, rare earth elements could react with H, O, N, C, S, Si, halogen, oxide and other nonmetallic impurities in aluminum melt to form compounds. So this reduced the content of gas content, inclusions and harmful elements in liquid aluminum, which achieved the role of gas removal, slag removal and matrix purification, and reduced porosity, porosity, slag inclusion and other defects in the ingot, so as to improve the quality of the ingot.

3.1. Sc

Sc had a very low solid solubility in Al-Zn-Mg-Cu alloy, and the presence of Sc led to the formation of primary Al₃Sc phase, which could act as the nucleating particle of Al matrix during solidification and significantly modify the as-cast structure [43]. Al₃Sc phase with different primary morphologies could produce different refining effects, which would affect the mechanical properties of the alloy. Holding at 760°C for 10 min followed by rapid cooling (at a cooling rate of 100-1000 K/s) could lead to the diversity of primary Al₃Sc phase morphology (Figure 9), and this form of Al-Sc alloy had the best refining effect on Al-Zn-Mg-Cu-Sc-Zr alloy [44].

Sc could not only affect the refining effect of Al-Zn-Mg-Cu alloy during solidification, but also could promote the uniform precipitation of η' phase during aging, which inhibited the coarsening of η' phase and prevented its transition to η phase [45]. Compared with 7055 aluminum alloy without Sc, the addition of 0.25% (mass fraction) of Sc made 7055 aluminum alloy smaller in size and it also made

η' phase distribution more uniform, so the alloy had higher hardness, tensile strength, ductility and thermal stability. Sc microalloying could improve the corrosion potential of aluminum alloy, thus improving the corrosion resistance [46]. The addition of trace Sc elements led to an increase in the proportion of grain boundaries in Al-Zn-Mg-Cu alloy, which reduced the amount of precipitated phase per unit grain boundary. Moreover, the discontinuous distribution of precipitated phase along grain boundaries greatly reduced the anodic dissolution rate of precipitated phase, which improved the resistance of the alloy to intergranular corrosion and spalling corrosion [47].

It had been shown that Sc also affected damping properties of Al-Zn-Mg-Cu alloys. The excellent damping performance of metal was due to the excellent grain boundary sliding ability of its crystal structure, and the fine grain structure always contributed to the improvement of grain boundary sliding ability. Therefore, the damping performance of Al-Zn-Mg-Cu alloy could be improved by refining the grain [48]. For example, reducing grain size, promoting the formation of equiaxed crystals and introducing wetting interface between Al-Zn phase, etc. [49]. 7055 alloy with 0.25% (mass fraction) Sc added was further treated by friction stir, which had fine grain and equiaxed fine crystal structure and showed the best damping performance [50].

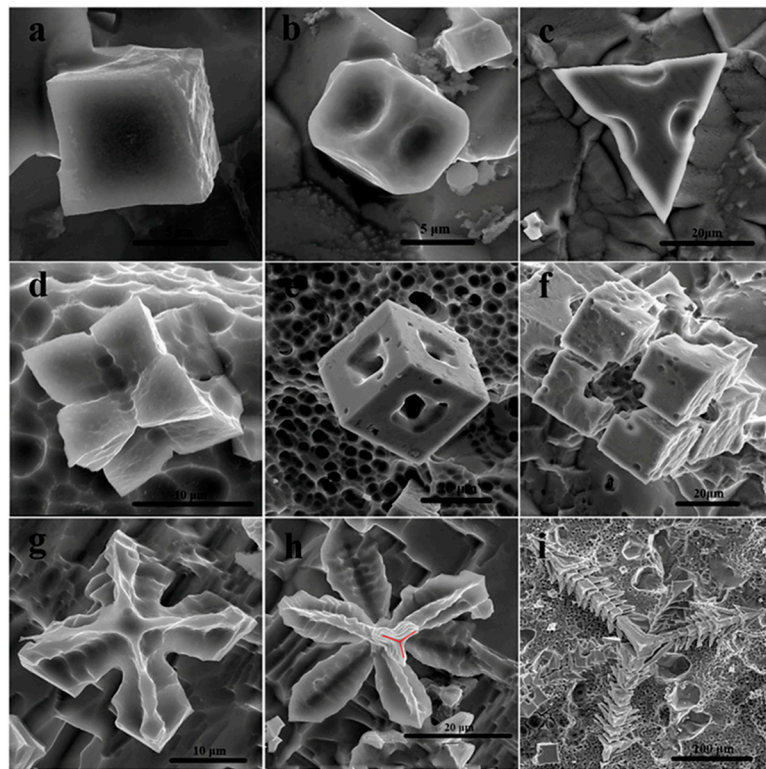


Figure 9. SEM images of primary particles which were obtained from as-cast Al-2.2Sc (wt.%) master alloy at the condition of melting temperature was 760 °C, holding time was 10 min, cooling rate was 100 to 1000 K/ s [44].

3.2. Zr

Adding 0.05% (mass fraction) Zr had no significant effect on grain refinement of Al-Zn-Mg-Cu alloy, but the Brinell hardness reached the maximum. With the increase of Zr content, the grain refinement effect became more obvious. When the addition amount reached 0.20% (mass fraction), the spacing between secondary dendrite arms reached the minimum, and the ultimate tensile strength, yield strength and elongation at room temperature reached the maximum 296.74MPa, 249.41MPa and 8.26%, respectively [51].

When Zr content was within a certain range, fine Al_3Zr dispersion phase could be formed to increase the number of crystal nuclei and refine grains [52]. For Al-Zn-Mg-Cu alloys with high cold-rolling ratio, the coherent interface between Al_3Zr particles and substrate changed to semi-coherent interface after solid solution treatment, which led to non-uniform nucleation of solutes during

quenching. So the quenched sensitivity increased that further increased with the cold rolling ratio. In contrast, Alloys with lower cold rolling ratios didn't show any significant quenching sensitivity [53].

3.3. Sc+Zr

The composite addition of trace Sc and Zr resulted in fine-grained strengthening, substructural strengthening, and Orowan mechanism strengthening of Al₃(Sc,Zr) and Al₃Zr dispersions [54]. By adding 0.07% (mass fraction) Sc and 0.07% (mass fraction) Zr, the strength of the alloy increased about 133 MPa. With the addition of 0.10% (mass fraction) Sc+0.16% (mass fraction) Zr and 0.22% (mass fraction) Sc+0.40% (mass fraction) Zr, Al-Zn-Mg-Cu alloy could obtain better recrystallization resistance and thermal stability. And with the increase of Sc and Zr addition, Abundant nano-Al₃(Sc,Zr) particles could effectively refine dislocations and subgrain boundaries, which showed good recrystallization resistance and precipitation strengthening effect [55].

The influence of Sc and Zr on the mechanical properties of Al-Zn-Mg-Cu alloys was mainly reflected in Al₃Sc and Al₃(Sc,Zr). Al₃Sc was the precursor of Al₃(Sc,Zr) precipitates. Saturated solid solutions containing Sc decomposed at 250 °C, which formed Sc-rich clusters and gradually developed into Al₃Sc crystal nuclei. With the increase of temperature, driven by the chemical potential gradient, Zr atoms began to diffuse over long distances and approached Al₃Sc nuclei. Then they enriched around them to form Zr-rich thin layers, thus forming the Al₃(Sc,Zr) core/shell structure of Al₃Sc crystal nuclei + Zr-rich shells [56]. The coarsening coefficient of Al₃(Sc,Zr) precipitates was 3 orders of magnitude smaller than that of Al₃Sc particles, which showed better thermal stability.

However, there was a threshold for the beneficial effect of Sc and Zr combined addition on yield strength. The addition of trace Sc and Zr improved the hardness and yield strength of 7055-T6 alloy by strengthening the grain boundary and Al₃(Sc,Zr) phase. But in Al-Zn-Mg-Cu alloy with high Cu content, Sc atoms diffused to θ-Al₂Cu phase, which promoted the formation of w-AlCuSc phase [57]. When the total mass fraction of Sc and Zr exceeded 0.45% (mass fraction), large w phase and coarse primary Al₃(Sc,Zr) phase were formed, leading to the degradation of mechanical properties of the alloy (Table 1) [58].

Table 1. Tensile properties of 7055-xZr-ySc alloy after rolling and T6 aging [58].

7055-xZr-ySc	Sc+Zr/wt. %	YS/Mpa	UTS/Mpa	EL/%
7055	0.16	577±2	654±2	12.8±0.4
7055-0.2Sc	0.36	609±2	649±3	13±0.5
7055-0.25Sc	0.41	600±2	679±2	14.3±0.5
7055-0.14Zr-0.15Sc	0.45	602±3	657±4	13.7±0.8
7055-0.14Zr-0.2Sc	0.5	593±3	635±5	10.3±0.6
7055-0.24Zr-0.15Sc	0.55	580±2	616±3	7.3±0.3

Note: (YS: Yield strength, UTS: Ultimate tensile strength, EL: Elongation).

3.4. Sm

Sm could effectively reduce the distance between secondary dendrite arms and was a good thinning element of aluminum alloy. The addition of Sm to Al-Cu alloy could refine the Al₂Cu phase in the alloy and promote its precipitation during aging [59]. The as-cast microstructure of Al-Zn-Mg-Cu-Zr alloy containing Sm mainly included η-(Mg(Zn,Cu,Al)₂) phases, Al₁₀Cu₇Sm₂ phases and Fe-rich phases, and there were also fine η phases and acicular θ(Al₂Cu) phases distributed in the grain [60]. The addition of Sm made the peak aging reach earlier and prolonged the peak aging time. With the increase of Sm content, the peak hardness of the alloy increased first and then decreased, and the maximum peak aging hardness was obtained at 0.3%Sm (mass fraction) [61].

The effect of Sm content on the ultimate tensile strength, yield strength and elongation of Al-Zn-Mg-Cu alloy at room temperature was similar, which firstly increased and then decreased. When the mass fraction of Sm reached 0.3%, the strengthening effect was the best, and the tensile strength, yield

strength and elongation were 732 MPa, 694 MPa and 9.3%, respectively. Compared with unmodified alloy, they were improved by 3.8%, 4.5% and 19%, respectively (Figure 10) [62].

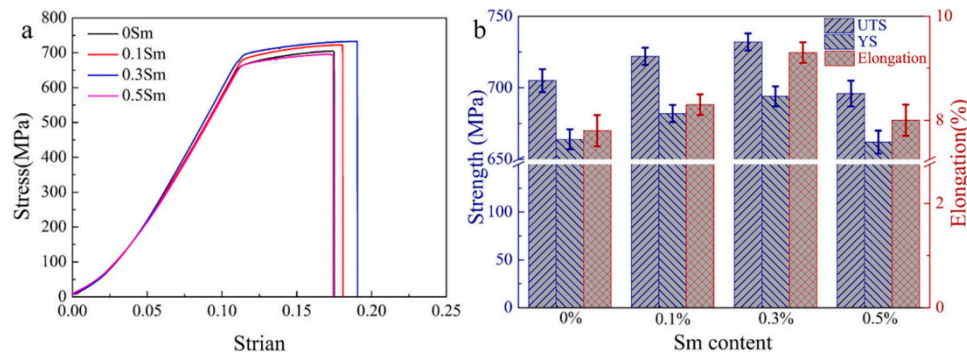


Figure 10. Tensile properties of the Al-Zn-Mg-Cu alloys with different Sm contents: (a) stress-strain curves, (b) relationship of ultimate tensile strength, yield strength and elongation with Sm contents [62].

3.5. Er

In Zr-containing Al-Zn-Mg-Cu alloys, Er and Zr could form dispersed $\text{Al}_3(\text{Er,Zr})$ phases [63]. $\text{Al}_3(\text{Er,Zr})$ phase could not only serve as the strengthening phase of matrix, but also nailed grain boundaries to inhibit the migration of low-angle grain boundaries to high-angle grain boundaries [64]. η phases tended to preferentially gather at the high Angle grain boundaries with higher energy, but the high Angle grain boundaries with abundant η phases were prone to anodic dissolution, which provided favorable channels for crack propagation [65]. Therefore, the addition of Er could preserve more low Angle grain boundaries, thus improving the corrosion resistance of the alloy. When the Er mass fraction increases from 0% (mass fraction) to 0.10% (mass fraction), the hardness and yield strength of the alloy increased by 25.4 HV and 70 MPa, respectively, and the intergranular corrosion depth decreased by 65% [66].

3.6. La

In Al-Zn-Mg-Cu alloys, Al-Ti-B was the most commonly used refiner. When La was added to aluminum alloys containing Al-Ti-B, La mainly existed in the form of $\text{Ti}_2\text{Al}_{20}\text{La}$ phase [67]. $\text{Ti}_2\text{Al}_{20}\text{La}$ phase was a non-thermodynamically stable phase [68], which could release rare earth elements. The rare earth could combine with TiB_2 particles to form "rare earth film", which reduced the free energy of TiB_2 phase and hindered the aggregation and growth of TiB_2 phase, thus maintaining the long-term refining ability of Al-Ti-B.

In addition, La atoms significantly promoted the nucleation and motion of di-slocation and could promote the twinning deformation at the crack tip, thus inhi-biting brittle propagation. Moreover, high concentration of La atoms was conduci-ve to promoting twin deformation and improving the plastic deformation ability o-f grain boundaries [69]. When 0.3% (mass fraction) of La was added into Al-6.7Zn-2.6Mg-2.0Cu-0.1Zr alloy, the tensile strength and yield strength were 583 MPa an-d 559 MPa, respectively, which were 18 MPa and 19 MPa higher than those wit-hout La modification [70].

3.7. Ce

Al-Zn-Mg-Cu alloys without Ce had a high degree of Cu susaturation, which would provide more Cu atoms to form Al_2CuMg phase, which resulted in a more stable Al_2CuMg particles. After adding 0.12%Ce (mass fraction), the stable AlCuCe phase could trap a large number of Cu atoms, effectively inhibit the further formation of Al_2CuMg phase [71], and it facilitated the dissolution of homogenization process. When Ce content increased to 0.3% (mass fraction), Al_4Ce phase appeared in the alloy [70]. In the process of solution treatment, fine Al_4Ce phase could nail the grain boundary, inhibit recrystallization and refine the structure.

In addition, adding Ce to Al-Zn-Mg aluminum alloy could significantly prolong the stress corrosion cracking time and reduce the stress corrosion sensitivity. When 0.04% (mass fraction) Ce was added to Al-Zn-Mg aluminum alloy, Ce atoms and Al atoms could be oxidized simultaneously to form rare-aluminum composite oxide film ($\text{Al}_2\text{O}_3\cdot\text{Ce}_2\text{O}_3$ and $(\text{Al,Ce})_2\text{O}_3$) [72], which improved the resistance of passivation film, significantly reduced the self-corrosion current density, and significantly improved the corrosion resistance of the alloy [73].

3.8. Y

The addition of 7.5% (mass fraction) Y in aluminum alloy could greatly improve the degree of grain refinement and dislocation density. And the formation of $\beta\text{-Al}_3\text{Y}$ intermetallic phases at grain boundaries could not only promoted nucleation, but also prevented grain growth, for which Al-7.5% (mass fraction) Y alloy could maintain fine grains in annealed state [74]. In 6063 aluminum alloy, the combined addition of rare earth Y and Al-Ti-B also played a role in reducing the grain size [75].

In Al-Zn-Mg-Cu alloys, adding Y element alone could refine dendrite substructure and increase the proportion of equiaxed crystals. The combined addition of Zr, Ti and Y could simultaneously refine the grain and dendrite substructure, and the tensile strength could reach about 700 MPa [76]. The synergistic strengthening of rare earth Y with transition elements Zr and Ti might be related to the formation of $\text{Al}_3\text{Cu}_4\text{Y}$ and $\text{Al}_3(\text{Zr,Y})$ phases in the nanonetwork structure. The ideal tensile strength of $\text{Al}_3\text{Cu}_4\text{Y}$ phase in (100) [001] slip system was 15.4 GPa [77], and it had good mechanical properties and thermal stability. The nanocrystalline $\text{Al}_3\text{Cu}_4\text{Y}$ phase was a more ideal existence form than the conventional $\text{Al}_3\text{Cu}_4\text{Y}$ phase. The strengthening of Al-Zn-Mg-Cu alloys had a wider application prospect.

3.9. Ta

The growth limiting factor Q value of Ta in aluminum alloy was 10.5K. It had been shown that the larger the Q value is, the more obvious the grain refinement effect is [78]. And Ta and Al had higher chemical activity and could form Al_3Ta phase in situ. The Al_3Ta phase with Al had small mismatch, which had been proven to be an efficient grain refiner for additive manufacturing [79].

Al-Zn-Mg-Cu alloy was prepared by laser powder bed melting (3D printing). The addition of 2% (mass fraction) Ta replaced Al atoms in the nano- Al_2Cu phase, and Al_3Ta and AlTaCu nanophases were formed by in-situ reaction, which prevented coarsening during solidification. These nanophases could inhibit hot cracking, refine and strengthen the alloy, and accelerate the aging process by hetero-nucleation or by hindering the oriented epitaxy growth of grains, thus increasing the ultimate tensile strength from 103 ± 21 MPa to 401 ± 11 MPa (Figure 11b). The aluminum alloy with Ta had a high Angle grain boundary, which could be used as a source of dislocation in the deformation process [80]. Therefore, the grain boundary surface of the alloy melted by laser powder bed had a high density of dislocation sources, which was conducive to deformation and thus to enhancing ductility. The addition of Ta transformed the fracture morphology from brittle intergranular fracture (Figure 11a) to ductile fracture (Figure 11c), and the elongation increased from $0.8\pm 0.4\%$ to $5.1\pm 0.6\%$. In addition, the discontinuous ultrafine grains and grain boundaries could inhibit the expansion of corrosion path, reduce the corrosion sensitivity of grain boundaries, and improve the Cl⁻ corrosion resistance of Al-Zn-Mg-Cu alloy [81].

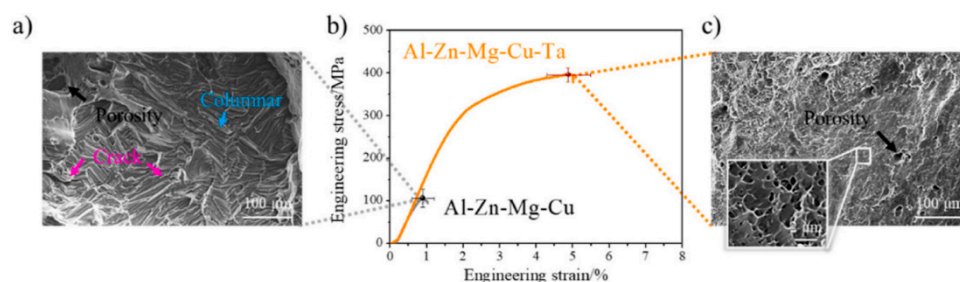


Figure 11. Tensile properties and fracture morphologies of the laser powder bed fusion-fabricated alloys: (a) fracture of Al–Zn–Mg–Cu, (b) stress-strain relations, and (c) fracture of Al–Zn–Mg–Cu–Ta [81].

4. Forecast

The effect of alloying on the microstructure and properties of Al-Zn-Mg-Cu alloy was reviewed. For the purpose of corrosion resistance, the ratio of Zn/Mg should be appropriately reduced to improve the corrosion resistance, and the content of Cu should be controlled to avoid the potential difference between grain boundary and Al matrix to cause the corrosion of precipitated phase. In order to achieve comprehensive energy, the iron-rich phase should be made as small as possible to reduce the adverse effects of impurity elements such as Fe and Si on plasticity and fracture toughness. By adding Sc, Zr and other rare earth elements, solution strengthening, aging strengthening and fine crystal strengthening should be introduced to improve the strength and toughness of the alloy. In addition, considering the machining properties of Al-Zn-Mg-Cu alloy, the quenching sensitivity of the alloy should be reduced by adding an appropriate amount of Ge element and the hot cracking tendency should be reduced by adding Ni element. According to the research status and existing problems of alloying Al-Zn-Mg-Cu alloy, the future research directions are as follows:

(1) Optimize the content of main alloy elements and control the content ratio of different main alloys, especially the content ratio of Zn/Mg to Zn/Cu. The influence mechanism of the main alloying elements on the microstructure and properties of Al-Zn-Mg-Cu alloy is studied deeply, and the action threshold of the main alloying elements is defined.

(2) Reduce the content of impurity elements to reduce the influence of impurity elements on the microstructure and properties of the alloy. The strength and toughness of the alloy can be improved by adding microalloying elements as needed, especially by adjusting the content of rare earth elements. The effects of precipitated phase content and distribution on the properties of Al-Zn-Mg-Cu alloys are analyzed and studied to improve the comprehensive mechanical properties of Al-Zn-Mg-Cu alloys to the greatest extent.

(3) Combining the effects of main alloying elements and trace alloying elements; the optimal alloying ratio of elements is analyzed through experimental tests; and the mechanism is explored to further optimize the microstructure and mechanical properties of the alloy.

Author Contributions: Investigation, Data curation, and Writing – original draft, J.W.; Project administration, Investigation, and Writing – revised, F.L.. All authors have read and agreed to the published version of the manuscript.

Funding: This research was funded by the Hunan Provincial Natural Science Foundation of China (No. 2021JJ30672), Science and Technology Project of Education Department of Hunan Province (No. 22A0100), College Students' innovation and entrepreneurship training program of Xiangtan University.

Institutional Review Board Statement: Not applicable.

Informed Consent Statement: Not applicable.

Data Availability Statement: Not applicable.

Acknowledgments: The authors gratefully acknowledge the support provided by Materials Intelligent Design College Students' Innovation and Entrepreneurship Education Center, Xiangtan University, Xiangtan, Hunan, China.

Conflicts of Interest: The authors declare no conflict of interest.

References

1. Chinh N.Q, Lendvai J, Ping D.H, et al. The effect of Cu on mechanical and precipitation prop-erties of Al-Zn-Mg alloys. *Journal of Alloys and Compounds*, **2004**, 378, 52. <https://doi.org/10.1016/j.jallcom.2003.11.175>
2. Dong P X, Chen S Y, Chen K H, et al. Effect of Cu content on microstructure and properties of super-high-strength Al-9.3Zn-2.4Mg-xCu-Zr alloy. *Journal of Alloys and Compounds*, **2019**, 788, 329. <https://doi.org/10.1016/j.jallcom.2019.02.228>

3. Zhao Y X, Li H, Liu Y, et al. The microstructures and mechanical properties of a highly alloyed Al-Zn-Mg-Cu alloy: The role of Cu concentration. *Journal of Materials Research and Technology*, **2022**, 18, 122. <https://doi.org/10.1016/j.jmrt.2022.02.071>
4. Huang R S, Li M N, Yang H F, et al. Effects of Mg contents on microstructures and second phases of as-cast Al-Zn-Mg-Cu alloys. *Journal of Materials Science & Technology*, **2022**, 21, 2105. <https://doi.org/10.1016/j.jmrt.2022.10.050>
5. Li H C, Cao F Y, Guo S, et al. Effects of Mg and Cu on microstructures and properties of spray-deposited Al-Zn-Mg-Cu alloy. *Journal of Alloys and Compounds*, **2017**, 719, 89. <https://doi.org/10.1016/j.jallcom.2017.05.101>
6. Shu W X, Hou L G, Zhang C, et al. Tailored Mg and Cu contents affecting the microstructures and mechanical properties of high-strength Al-Zn-Mg-Cu alloys. *Materials Science and Engineering: A*, **2016**, 657, 269. <https://doi.org/10.1016/j.msea.2016.01.039>
7. Tang J, Liu M C, Bo G W, et al. Unraveling precipitation evolution and strengthening function of the Al-Zn-Mg-Cu alloys with various Zn contents: Multiple experiments and integrated internal-state-variable modeling. *Journal of Materials Science & Technology*, **2022**, 116, 130. <https://doi.org/10.1016/j.jmst.2021.12.008>
8. Tan P, Sui Y D, Jin H N, et al. Effect of Zn content on the microstructure and mechanical properties of as-cast Al-Zn-Mg-Cu alloy with medium Zn content. *Journal of Materials Research and Technology*, **2022**, 18, 2620. <https://doi.org/10.1016/j.jmrt.2022.03.168>
9. Curle U A, Cornish L A, Govender G. Predicting yield strengths of Al-Zn-Mg-Cu-(Zr) aluminium alloys based on alloy composition or hardness. *Materials & Design*, **2016**, 99, 211. <https://doi.org/10.1016/j.matdes.2016.03.071>
10. Tang J, Zhang H, Teng J, et al. Effect of Zn content on the static softening behavior and kinetics of Al-Zn-Mg-Cu alloys during double-stage hot deformation. *Journal of Alloys and Compounds*, **2019**, 806, 1081. <https://doi.org/10.1016/j.jallcom.2019.07.332>
11. Tang J, Wang J H, Teng J, et al. Effect of Zn content on the dynamic softening of Al-Zn-Mg-Cu alloys during hot compression deformation. *Vacuum*, **2021**, 184, 109941. <https://doi.org/10.1016/j.vacuum.2020.109941>
12. Xu Y T, Zhang Z F, Gao Z H, et al. Effect of main elements (Zn-Mg and Cu) on the microstructure, castability and mechanical properties of 7xxx series aluminum alloys with Zr and Sc. *Materials Characterization*, **2021**, 182, 111559. <https://doi.org/10.1016/j.matchar.2021.111559>
13. Zhang Z R, Li Y, Li H X, et al. Effect of high Cu concentration on the mechanical property and precipitation behavior of Al-Mg-Zn-(Cu) crossover alloys. *Journal of Materials Science & Technology*, **2022**, 20, 4585. <https://doi.org/10.1016/j.jmrt.2022.08.171>
14. Wei S L, Wang R C, Zhang H, et al. Influence of Cu/Mg ratio on microstructure and mechanical properties of Al-Zn-Mg-Cu alloys. *Journal of Materials Science*, **2021**, 56, 3472. <https://doi.org/10.1007/s10853-020-05438-0>
15. Chung T F, Yang Y L, Huang B M, et al. Transmission electron microscopy investigation of separated nucleation and in-situ nucleation in AA7050 aluminium alloy. *Acta Materialia*, **2018**, 149, 377. <https://doi.org/10.1016/j.actamat.2018.02.045>
16. Hou S L, Liu P P, Zhang D, et al. Precipitation hardening behavior and microstructure evolution of Al-5.1Mg-0.15Cu alloy with 3.0Zn (wt %) addition. *Journal of Materials Science*, **2018**, 53, 3846. <https://doi.org/10.1007/s10853-017-1811-1>
17. Zou Y, Wu X D, Tang S B. Investigation on microstructure and mechanical properties of Al-Zn-Mg-Cu alloys with various Zn/Mg ratios. *Journal of Materials Science & Technology*, **2021**, 85, 106. <http://doi.org/10.1016/j.jmst.2020.12.045>
18. Liu S C, Xu G F, Li Y, et al. The Influence of the Zn/Mg ratio on the quench sensitivity of Al-Zn-Mg-Cu alloys. *Journal of Materials Engineering and Performance*. **2020**, 29, 5787. <https://doi.org/10.1016/j.actamat.2020.29.5787>
19. Graf G, Spoerk-Erdely P, Staron P, et al. Quench rate sensitivity of age-hardenable Al-Zn-Mg-Cu alloys with respect to the Zn/Mg ratio: An in situ SAXS and HEXRD study. *Acta Materialia*, **2022**, 227, 117727. <https://doi.org/10.1016/j.actamat.2022.117727>
20. Zhang C L, Lv P, Cai J, et al. Enhanced corrosion property of W-Al coatings fabricated on aluminum using surface alloying under high-current pulsed electron beam. *Journal of Alloys and Compounds*, **2017**, 723, 258. <https://doi.org/10.1016/j.jallcom.2017.06.189>
21. Li C, Xu X J, Chen H H, et al. Effect of Zn/Mg ratio on microstructure and properties of cold extruded Al-xZn-2.4Mg-0.84Cu-0.2Zr-0.25Ti aluminum alloy. *Journal of Materials Engineering and Performance*, **2020**, 29, 5787. <http://doi.org/10.1007/s11665-020-05096-y>
22. Li X M, Starink M J. Identification and analysis of intermetallic phases in overaged Zr-containing and Cr-containing Al-Zn-Mg-Cu alloys. *Journal of Alloys and Compounds*, **2011**, 509, 471. <http://doi.org/10.1016/j.jallcom.2010.09.064>

23. Guo E J, Li Z H, Lv X Y, et al. Research on microstructure in as-cast 7A55 aluminum alloy and its evolution during homogenization. *Rare Metals*, **2011**, 30, 664. <https://doi.org/10.1007/s12598-011-0446-7>
24. Morgeneyer T F, Starink M J, Sinclair I. Evolution of voids during ductile crack propagation in an aluminium alloy sheet toughness test studied by synchrotron radiation computed tomography. *Acta Materialia*. **2008**, 56, 1671. <http://doi.org/10.1016/j.actamat.2007.12.019>
25. Vratnica M, Pluvina G, Jodin P, et al. Influence of notch radius and microstructure on the fracture behavior of Al-Zn-Mg-Cu alloys of different purity. *Materials & Design*, **2010**, 31, 1790. <http://doi.org/10.1016/j.matdes.2009.11.018>
26. Ohira T, Kishi T. Effect of iron content on fracture toughness and cracking processes in high strength Al-Zn-Mg-Cu alloy. *Materials Science and Engineering*. **1986**, A78, 9. [http://doi.org/10.1016/0025-5416\(86\)90075-3](http://doi.org/10.1016/0025-5416(86)90075-3)
27. Hu K, Lin C H, Xi S C, et al. Effect of Fe content on low cycle fatigue behavior of squeeze cast Al-Zn-Mg-Cu alloys. *Materials Characterization*, **2020**, 170, 110680. <http://doi.org/10.1016/j.matchar.2020.110680>
28. Kovarik K, Court S A, Fraser H L, et al. GPB zones and composite GPB/GPBII zones in Al-Cu-Mg alloys. *Acta Materialia*, **2008**, 56, 4804. <http://doi.org/10.1016/j.actamat.2008.05.042>
29. Guo K H, Liang S S, Wen S P, et al. GPB-II zone in Si microalloyed Al-Zn-Mg-Cu alloy and its strengthening effect. *Materials Science & Engineering A*, **2022**, 852, 143721. <https://doi.org/10.1016/j.msea.2022.143721>
30. Zeng X H, Xue P, Wu L H, et al. Microstructural evolution of aluminum alloy during friction stir welding under different tool rotation rates and cooling conditions. *Journal of Materials Science & Technology*, **2019**, 35, 972. <http://doi.org/10.1016/j.jmst.2019.35.972>
31. She H, Shu D, Dong A P, et al. Relationship of particle stimulated nucleation, recrystallization and mechanical properties responding to Fe and Si contents in hot-extruded 7055 aluminum alloys. *Journal of Materials Science & Technology*, **2019**, 35, 2570. <http://doi.org/10.1016/j.jmst.2019.07.014>
32. Zhu Q Q, Cao L F, Wu X D, et al. Effect of Ag on age-hardening response of Al-Zn-Mg-Cu alloys. *Materials Science & Engineering A*, **2019**, 754, 265. <https://doi.org/10.1016/j.msea.2019.03.090>
33. Wang Y C, Wu X D, Cao L F, et al. Effect of Ag on aging precipitation behavior and mechanical properties of aluminum alloy 7075. *Materials Science & Engineering A*, **2021**, 804, 140515. <https://doi.org/10.1016/j.msea.2020.140515>
34. Wang S, He C, Luo B H, et al. The role of trace Ag in controlling the precipitation and stress corrosion properties of aluminium alloy 7N01. *Vacuum*, **2021**, 184, 109948. <https://doi.org/10.1016/j.vacuum.2020.109948>
35. Lin L H, Liu Z Y, Bai S, et al. Effects of Ge and Ag additions on quench sensitivity and mechanical properties of an Al-Zn-Mg-Cu alloy. *Materials Science & Engineering A*, **2017**, 682, 640. <https://doi.org/10.1016/j.msea.2016.11.092>
36. Naeem H T, Mohammed K S, Ahmad K R, et al. The influence of nickel and tin additives on the microstructural and mechanical properties of Al-Zn-Mg-Cu Alloys. *Advances in Materials Science and Engineering*, **2014**, 686474. <https://doi.org/10.1155/2014/686474>
37. Akopyan T K, Padalko A G, Belov N A, et al. Effect of barothermal treatment on the structure and the mechanical properties of a high-strength eutectic Al-Zn-Mg-Cu-Ni aluminum alloy. *Russian Metallurgy (Metally)*, **2017**, 922. <http://doi.org/10.1134/S0036029517110027>
38. Liu F C, Zhu X Z, Ji S X, Effects of Ni on the microstructure, hot tear and mechanical properties of Al-Zn-Mg-Cu alloys under as-cast condition. *Journal of Alloys and Compounds*, **2020**, 821, 153458. <https://doi.org/10.1016/j.jallcom.2019.153458>
39. Zeng X C, Ferguson C, Shankar S. Effect of Titanium levels on the hot tearing sensitivity and abnormal grain growth after T4 treatment of Al-Zn-Mg-Cu alloys. *International Journal of Metalcasting*, **2018**, 12, 457. <http://doi.org/10.1016/i.jmetal.2018.12.457>
40. Lee S-H, Jung J-G, Baik S-I, et al, Effects of Ti addition on the microstructure and mechanical properties of Al-Zn-Mg-Cu-Zr alloy. *Materials Science & Engineering A*, **2021**, 801, 140437. <http://doi.org/10.1016/j.msea.2020.140437>
41. Kayani S H, Jung J G, Kim M S, et al. Effect of cooling rate on precipitation behavior of Al-65Zn-2.59Mg-1.95Cu alloy with minor elements of Zr and Ti. *Metals and Materials International*, **2020**, 26, 1079. <http://doi.org/10.1007/s12540-019-00385-1>
42. Lee S H, Kayani S H, Jung J G, et al. Crystallographic characterization of Al₁₈Mg₃Ti₂ intermetallic phase in Al-Zn-Mg-Cu-Zr-Ti alloy. *Journal of Alloys and Compounds*, **2020**, 844, 156173. <http://doi.org/10.1016/j.jallcom.2020.156173>
43. Ying T, Gu L D, Tang X Y, et al. Effect of Sc microalloying on microstructure evolution and mechanical properties of extruded Al-Zn-Mg-Cu alloys. *Materials Science & Engineering A*, **2022**, 831, 142197. <https://doi.org/10.1016/j.msea.2021.142197>

44. Sun Y Q, Pan Q L, Luo Y H, et al. Study on the primary Al₃Sc phase and the structure heredity of Al-Zn-MgCu-Sc-Zr alloy. *Materials Characterization*, **2020**, 169, 110601. <http://doi.org/10.1016/materials.2020.169.110601>
45. Teng G B, Liu C Y, Ma Z Y, et al. Effects of minor Sc addition on the microstructure and mechanical properties of 7055 Al alloy during aging. *Materials Science & Engineering A*, **2018**, 713, 61. <https://doi.org/10.1016/j.msea.2017.12.067>
46. Mondol S, Alam T, Banerjee R, et al. Development of a high temperature high strength Al alloy by addition of small amounts of Sc and Mg to 2219 alloy. *Materials Science and Engineering: A*, **2017**, 687, 221. <https://doi.org/10.1016/j.msea.2017.01.037>
47. Sun Y Q, Luo Y H, Pan Q L, et al. Effect of Sc content on microstructure and properties of Al-Zn-Mg-Cu-Zr alloy. *Materials Today Communications*, **2021**, 26, 101899. <https://doi.org/10.1016/j.mtcomm.2020.101899>
48. Luo B H, Bai Z H, Xie Y Q. The effects of trace Sc and Zr on microstructure and internal friction of Zn-Al eutectoid alloy. *Materials Science and Engineering: A*, **2004**, 370, 172. <https://doi.org/10.1016/j.msea.2002.12.007>
49. Jiang H J, Liu C Y, Ma Z Y, et al. Fabrication of Al-35Zn alloys with excellent damping capacity and mechanical properties. *Journal of Alloys and Compounds*. **2017**, 722, 138. <https://doi.org/10.1016/j.jallcom.2017.06.091>
50. Chen Y., Liu C H, Zhang B, et al. Effects of friction stir processing and minor Sc addition on the microstructure, mechanical properties, and damping capacity of 7055 Al alloy. *Materials Characterization*, **2018**, 135, 25. <https://doi.org/10.1016/j.matchar.2017.11.030>
51. Yang Y, Tan P, Sui Y D, et al. Influence of Zr content on microstructure and mechanical properties of As-cast Al-Zn-Mg-Cu alloy. *Journal of Alloys and Compounds*, **2021**, 867, 158920. <https://doi.org/10.1016/j.jallcom.2021.158920>
52. Cassell A M, Robson J D, Race C P, et al. Dispersoid composition in zirconium containing Al-Zn-Mg-Cu (AA7010) aluminium alloy. *Acta Materialia*, **2019**, 169, 135. <https://doi.org/10.1016/j.actamat.2019.02.047>
53. Pan T A, Tzeng Y C, Bor H Y, et al. Effects of the coherency of Al₃Zr on the microstructures and quench sensitivity of Al-Zn-Mg-Cu alloys. *Materials Today Communications*, **2021**, 28, 102611. <https://doi.org/10.1016/j.mtcomm.2021.102611>
54. Xiao Q F, Huang J W, Jiang Y G, et al. Effects of minor Sc and Zr additions on mechanical properties and microstructure evolution of Al-Zn-Mg-Cu alloys. *Transactions of Nonferrous Metals Society of China*, **2020**, 30, 1429. [https://doi.org/10.1016/S1003-6326\(20\)65308-0](https://doi.org/10.1016/S1003-6326(20)65308-0)
55. Liu J, Yao P, Zhao N Q, et al. Effect of minor Sc and Zr on recrystallization behavior and mechanical properties of novel Al-Zn-Mg-Cu alloys. *Journal of Alloys and Compounds*, **2016**, 657, 717. <https://doi.org/10.1016/j.jallcom.2015.10.122>
56. Wang Y, Xiong B Q, Li Z H, et al. Precipitation behavior of Al₃(Sc,Zr) particles in high-alloyed Al-Zn-Mg-Cu-Zr-Sc alloy during homogenization. *Arabian Journal for Science and Engineering*, **2021**, 46, 6027. <https://doi.org/10.1007/s13369-020-05268-x>
57. Jia M, Zheng Z Q, Gong Z. Microstructure evolution of the 1469 Al-Cu-Li-Sc alloy during homogenization. *Journal of Alloys and Compounds*, **2014**, 614, 131. <https://doi.org/10.1016/j.jallcom.2014.06.033>
58. Liu C Y, Teng G B, Ma Z Y. Effects of Sc and Zr microalloying on the microstructure and mechanical properties of high Cu content 7xxx Al alloy. *International Journal of Minerals, Metallurgy and Materials*, **2019**, 26, 1559. <http://doi.org/10.1007/s12613-019-1840-7>
59. Li Z, Hu Z, Yan H. Effect of Samarium(Sm) addition on microstructure and mechanical properties of Al-5Cu alloys. *Journal of Wuhan University of Technology Mater, Sci. ed*, **2016**, 31, 624. <http://doi.org/10.1007/s11595-016-1420-x>
60. Zhai F L, Wang L P, Gao X. Phase evolution of a novel Al-Zn-Mg-Cu-Zr-Sm alloy during homogenization annealing treatment. *Materials Research Express*, **2020**, 7, 076518. <http://doi.org/10.1088/2053-1591/aba6bf>
61. Zhai F L, Wang L P, Gao X, et al. Effect of samarium on the high temperature tensile properties and fracture behaviors of Al-Zn-Mg-Cu-Zr alloy. *Materials Research Express*, **2021**, 8, 01652. <http://doi.org/10.1088/2053-1591/abd89b>
62. Zhai F L, Fan R, Feng Y C, et al. Effect of samarium modification on the microstructures evolution and mechanical properties of high strength aluminum alloy. *Materials Characterization*, **2022**, 194, 112349. <https://doi.org/10.1016/j.matchar.2022.112349>
63. Fang H C, Chao H, Chen K H. Effect of Zr, Er and Cr additions on microstructures and properties of Al-Zn-Mg-Cu alloys. *Materials Science & Engineering A*, **2014**, 610, 10. <https://doi.org/10.1016/j.msea.2014.05.021>
64. Zhong H L, Li S C, Zhang Z Q, et al. Precipitation behavior, mechanical properties, and corrosion resistance of rare earth-modified Al-Zn-Mg-Cu alloys. *Materials Today Communications*, **2022**, 31, 103732. <https://doi.org/10.1016/j.mtcomm.2022.103732>

65. Krishnan A, Raja V S, Mukhopadhyay A K. Influence of retrogression and Reaging on the exfoliation corrosion behavior of AA 7085 sheets. *Corrosion Science and Technology*, **2016**, 15, 159. <http://doi.org/10.14773/cst.2016.15.4.159>
66. Wang Y C, Wu X D, Cao L F, et al. Effect of trace Er on the microstructure and properties of Al–Zn–Mg–Cu–Zr alloys during heat treatments. *Materials Science & Engineering A*, **2020**, 792, 139807. <https://doi.org/10.1016/j.msea.2020.139807>
67. Chen Z Q, Hu W X, Shi L, et al. Effect of rare earth on morphology and dispersion of TiB₂ phase in Al–Ti–B alloy refiner. *China Foundry*, **2023**, 20, 115. <https://doi.org/10.1007/s41230-023-2113-7>
68. Yin D S, Zhang N, Chen K J, et al. Effect of Gd on microstructure and refinement performance of Al–5Ti–B alloy. *China Foundry*, **2021**, 18, 223. <http://doi.org/10.1007/s41230-023-2113-7>
69. Wang Z P, Xiao H, Ma L, et al. Effects of rare-earth elements on twinning deformation of Al alloys from first-principles calculations. *Solid State Communications*, **2022**, 356, 114946. <https://doi.org/10.1016/j.ssc.2022.114946>
70. Zhai F L, Wang L P, Gao X. Study on phases formation and modification ability of rare earth elements La, Ce, Sm and Er in Al–Zn–Mg–Cu–Zr alloy. *Transactions of The Indian Institute of Metals*, **2021**, 74, 2639. <http://doi.org/10.1007/s12666-021-02337-z>
71. Yu X X, Sun J, Li Z T, et al. Solidification behavior and elimination of undissolved Al₂CuMg phase during homogenization in Ce-modified Al–Zn–Mg–Cu alloy. *Rare Metals*, **2020**, 39, 1279. <http://doi.org/10.1007/s12598-018-1172-1>
72. Michalik Rafał, Woźnica H. The effect of Ti and REE addition on the corrosion resistance of the AlZn12Mg3.5Cu2.5 alloy in “acid rain” environment. *Solid State Phenomena*, **2015**, 227, 111. <https://doi.org/10.4028/www.scientific.net/SSP.227.111>
73. Hu G Y, Zhu C J, Xu D F. Effect of cerium on microstructure, mechanical properties and corrosion properties of Al–Zn–Mg alloy. *Journal of Rare Earths*, **2021**, 39, 208. <https://doi.org/10.1016/j.jre.2020.07.010>
74. Wang M M, Knezevic M, Chen M, et al. Microstructure design to achieve optimal strength, thermal stability, and electrical conductivity of Al–7.5wt.%Y alloy. *Materials Science & Engineering A*, **2022**, 852, 143700. <https://doi.org/10.1016/j.msea.2022.143700>
75. Ding W W, Zhao X Y, Chen T L, et al. Effect of rare earth Y and Al–Ti–B master alloy on the microstructure and mechanical properties of 6063 aluminum alloy. *Journal of Alloys and Compounds*, **2020**, 830, 154685. <https://doi.org/10.1016/j.jallcom.2020.154685>
76. Li J H, Zhang Y B, Li M J, et al. Effect of combined addition of Zr, Ti and Y on microstructure and tensile properties of an Al–Zn–Mg–Cu alloy. *Materials & Design*, **2022**, 223, 111129. <https://doi.org/10.1016/j.matdes.2022.111129>
77. Yang W, Pang M, Tan Y, et al. A comparative first-principles study on electronic structures and mechanical properties of ternary intermetallic compounds Al₈Cr₄Y and Al₈Cu₄Y: Pressure and tension effects. *Journal of Physics and Chemistry of Solids*, **2016**, 98, 298. <https://doi.org/10.1016/j.jpcs.2016.07.008>
78. Zhang D, Qiu D, Gibson M A, et al. Additive manufacturing of ultrafine-grained high-strength titanium alloys. *Nature*, **2019**, 576, 91. <https://doi.org/10.1038/s41586-019-1783-1>
79. Martin J H, Yahata B, Mayer J, et al. Grain refinement mechanisms in additively manufactured nano-functionalized aluminum. *Acta Materialia*, **2020**, 200, 1022. <https://doi.org/10.1016/j.actamat.2020.09.043>
80. Straumal B B, Baretzky B, Mazilkin A A, et al. Formation of nanogained structure and decomposition of supersaturated solid solution during high pressure torsion of Al–Zn and Al–Mg alloys. *Acta Materialia*, **2004**, 52, 4469. <https://doi.org/10.1016/j.actamat.2004.06.006>
81. Li X W, Li D W, Li G, et al. Microstructure, mechanical properties, aging behavior, and corrosion resistance of a laser powder bed fusion fabricated Al–Zn–Mg–Cu–Ta alloy. *Materials Science & Engineering A*, **2022**, 832, 142364. <https://doi.org/10.1016/j.msea.2021.142364>

Disclaimer/Publisher’s Note: The statements, opinions and data contained in all publications are solely those of the individual author(s) and contributor(s) and not of MDPI and/or the editor(s). MDPI and/or the editor(s) disclaim responsibility for any injury to people or property resulting from any ideas, methods, instructions or products referred to in the content.